# Polarization effect on *p*-type doping efficiency in Mg-Si codoped wurtzite GaN from first-principles calculations

Jinchai Li and Junyong Kang*
*Department of Physics, Pen Tung Sah MEMS Research Center, and Semiconductor Photonics Research Center, Xiamen University, Xiamen 361005, People's Republic of China*
(Received 26 June 2004; published 28 January 2005)

The electronic structures of two Mg-Si codoped configurations in wurtzite GaN were calculated by an *ab initio* "mixed-basis + norm conserving nonlocal pseudopotential" method. The results show that the charge densities redistribute and concentrate in the N-Mg bonds for the configuration with a local polarized field component that strengthens the polarizability. The tops of the valence bands are thus split widely and shifted up towards the conduction band. The N atoms bonding to the Mg atom are found to be as important as the Mg atom for the formation of the tops of the valence band. These electronic structure shifts can enhance the hole concentration about $10^3$ times higher than that of Mg-doped GaN.

DOI: 10.1103/PhysRevB.71.035216 PACS number(s): 61.72.Vv, 77.22.Ej, 71.20.Nr

## I. INTRODUCTION

The wide, direct energy band gap and good thermal stability of GaN make it suitable for short wavelength emitters, detectors, high-temperature and high-power electronics.[1–3] The highly conductive property of *p*-type GaN is especially important for optical and electrical devices.[4] Magnesium is an effective acceptor impurity for group-III nitrides.[5–7] Experimental results, however, show that as the Mg concentration in the films is increased, the hole concentration eventually saturates and decreases.[8] Furthermore, the high activation energy of Mg may also limit the formation of acceptors.[4,9] Theoretical and experimental research has been performed to enhance the hole concentration, and a codoping mechanism has been discussed.[9–11] Recently, Iwai *et al.* have obtained a high hole concentration of $2\times10^{19}$ cm$^{-3}$ and a low acceptor activation energy for *p*-type GaN by introducing Mg and Si sources alternatively.[4] However, the reason the codoping method can significantly enhance the hole concentration still awaits clarification.

One important difference of wurtzite GaN from the traditional III-V semiconductors is the polarization of the structure. Mg and Si impurities usually substitute for the Ga host atoms, and their valence difference will change the local polarity. The local polarity then depends on the substitutional configuration of the Mg-Si codopants. Therefore, it is necessary to investigate the polarity effect on *p*-type doping efficiency in Mg-Si codoped wurtzite GaN.

## II. CALCULATION DETAILS

Two substitutional configurations in a 32-atom wurtzite supercell were constructed to simplify calculation. The two configurations are a substitution of Si into a Ga site as the second-neighbor above and below Mg, denoted as I and II in Fig. 1, respectively. The Mg impurity is fixed in one of the 16 substitutional Ga sites. Therefore, the local polarized field in configuration I strengthens the polarizability, but it is weakened for configuration II.

The calculations were performed by employing an *ab initio* "mixed-basis + norm conserving nonlocal pseudopotential" method, which has been well tested in solid-state physics calculations. The Ceperly-Alder formula was adopted to form the exchange and correlation energy. The plane-wave cutoff energy was set to 17 Ry, and other parameters were set the same as our previous calculation.[12]

As a basis for Mg-Si codoped GaN, the equilibrium lattice constant of the undoped wurtzite GaN supercell was found to be $a_0=0.303$ nm by using a first-principles total-energy calculation, and $c_0/a_0$ ratio was taken as equal to the ideal value, 1.63299. The charge density distribution and the total density of states (DOS) of undoped and Mg-doped GaN were then calculated with and without lattice relaxations. The acceptor level does not appear in the energy band gap, and the Mg-nearest-neighbor N bonds relax 5.22% and 4.67% outward along the *c* axis and the rest bonding directions, respectively. These results agree with previous literature studies.[4,10,13] The Mg-Si codoped calculations are performed as below.

## III. RESULTS AND DISSCUSSIONS

The charge density distributions of different layers for both confirations I and II were calculated and compared with

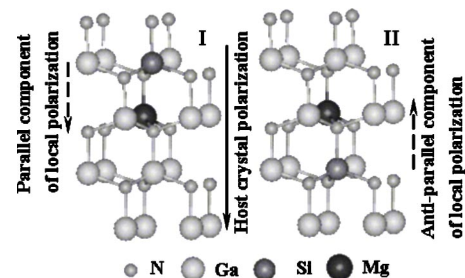


FIG. 1. Crystal structures of supercells of Mg-Si codoped wurtzite GaN for configurations I and II. The polarization orientation in the host crystals is marked with a solid arrow, and the local polarization components induced by Mg and Si codoped configurations are marked with the dashed ones.

 ©2005 The American Physical Society

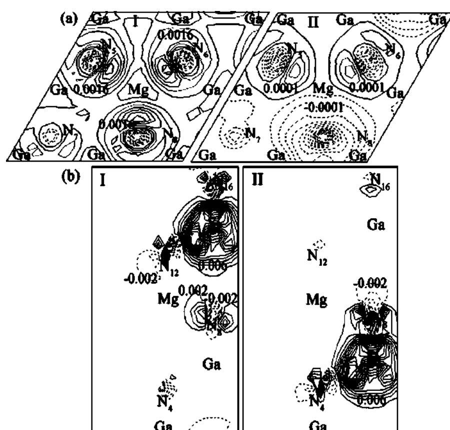

FIG. 2. Charge density distribution differences on an *ab*-plane containing the Mg atom (a) and on a cross section containing Mg and Si atoms (b), obtained by subtracting the charge density of Mg doped from those of configurations I and II, respectively. The negative and positive data are shown by the dashed and solid curves, respectively.

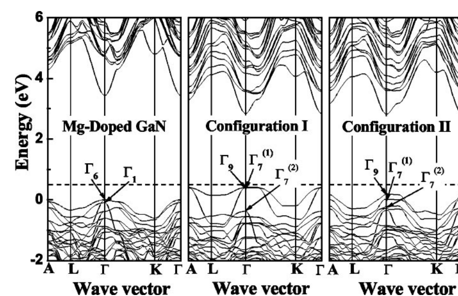


FIG. 3. Energy band structures of the Mg-doped GaN, configurations I and II. The dashed line in the band gap is assumed to be an Mg-related acceptor level.

those of Mg-doped GaN. To reveal their difference, we subtracted the charge density distribution of Mg-doped GaN from that of both confirations I and II. The results are shown in Fig. 2(a) for an *ab* plane containing the Mg atom. The subtracted values are negative in the central regions above the N atoms bonding to Mg atom. In the outer regions, by contrast, they are positive for all three N atoms in configuration I and for two of the three in configuration II. This indicates the redistributions of the electron clouds for the N atoms bonding to Mg. In particular, the electron clouds concentrate on the sides near the Mg atom. This shows that the codoped crystals favor strengthening some N-Mg bonds.

The strengthening effect is more obvious by comparing the N atoms with the Si impurities above and below, denoted as $N_8$ in Fig. 2(a). Figure 2(b) displays the difference of charge density distributions of a Mg-doped crystal from a cross section containing Mg and Si atoms. This shows the influence of the Si impurity. The charge densities of Si atoms are much higher in both codoped crystals. This is not only because the valence of Si is one larger than that of Ga, but also because the electronegativity[14] of Si (1.8) is larger than that of Ga (1.6). This leads to sparse electron distributions at the N ends of the bonds with Si atoms (such as $N_{12}$ and $N_{16}$ of configuration I, $N_4$ and $N_8$ of configuration II). At the same time, the electrons distribute more densely in other directions. In configuration I, this means that more electrons concentrate at the N ends of the bonds with Mg and further enhance the local polarized field around the Mg atom. In configuration II, the cloud changes are less around Mg.

Because the symmetry of the electron clouds around Mg for both configurations I and II changes, the energy band structures are clearly influenced. The calculated results (Fig. 3) show the band structure contrast between Mg-doped and both configurations I and II, especially the splitting and shifts of the tops of the valence bands ($E_\nu$). The doubly degenerate $\Gamma_{6\nu}$ level near $E_\nu$ splits into $\Gamma_{9\nu}$ and $\Gamma_{7\nu}^{(1)}$ levels. The singly degenerate $\Gamma_{1\nu}$ level is labeled $\Gamma_{7\nu}^{(2)}$. The energy difference between $\Gamma_{9\nu}$ level and $\Gamma_{7\nu}^{(2)}$ level $\Delta E = E(\Gamma_{9\nu}) - E(\Gamma_{7\nu}^{(2)}) = 0.791$ eV of configuration I is much larger than 0.409 eV of configuration II. The energy differences of $\Delta E$ for configurations I and II, respectively, shifts $E_\nu$ by values 0.423 eV and 0.192 eV higher than that in Mg-doped GaN at the $\Gamma$ point. Meanwhile, the bottoms of the conduction bands ($E_c$) of configuration I and II shift lower than that of Mg-doped GaN, which might be induced by the Si dopant. $E_c$ of configuration I is 0.03 eV higher than that of configuration II, indicating that the effect of the *n*-type Si dopant is weaker for configuration I. If there is a Mg-related acceptor level near $E_\nu$, its activation energy will be lower for configuration I. Therefore, the *p*-type doping efficiency of configuration I is believed to be higher than that of configuration II.

Because the *ab initio* "mixed-basis + norm conserving nonlocal pseudopotential" method does not take the spin-orbit interaction into account, the difference of the splitting energy near $E_\nu$ is related to the crystal field difference between configuration I and II. It is known that there is a lack of one valence electron around Mg in the substitutional Ga site, and a local positive center is formed. On the other hand, Si in the substitutional Ga site has one additional valence electron and forms a local negative center. The local negative and positive centers generate a local polarized field. The local polarized field can be decomposed into two components, one along the *c* axis and the other perpendicular to the *c* axis. The orientations and magnitudes of the perpendicular components are nearly the same for configurations I and II. However, the *c*-axis component is parallel and antiparallel to the polarized field of the host crystal for the two cases, respectively, as indicated in Fig. 1. The parallel component strengthens the polarizability and the antiparallel component weakens it. Based on the above analysis, we conclude the larger energy difference $\Delta E$ is mainly attributable to the increase of the polarizability for configuration I.

In order to understand the contributions of different atoms to the shifts of $E_\nu$, the total and partial DOS were calculated and compared. As the total DOS results show in Fig. 4(a), the splitting band produces dense states around the valence band edge for configuration I. This enhances the electron transition probability from the Mg-related acceptor level to the valence band. Generally, a *p*-type Mg dopant is considered responsible for the formation of the states around the valence band edge. This does not occur in Mg-doped GaN but does occur in *p*-type Mg and *n*-type Si codoped GaN. It is therefore necessary to examine the role of each atom by

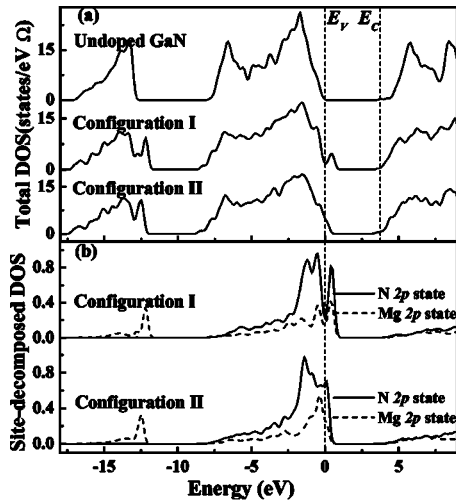


FIG. 4. Total (a) and site-decomposed DOS (b) of the undoped GaN, configurations I and II.

studying the site-decomposed DOS. The $2p$ states of Mg and its bonding N atoms are found to be much denser than other atoms around the valence band edge, as a typical site-decomposed DOS shows in Fig. 4(b). Furthermore, the $2p$ states of the N and Mg atoms strongly shift toward the conduction band for configuration I. From this point of view, the N atoms play an important role as well as the Mg atom in the formation of the energy states around the valence band edge. This is done by redistributing more electrons along N-Mg bonds, strengthening their bonds due to an increase of local polarizability, as mentioned above.

The hole concentration in a semiconductor with acceptor only near absolute zero is given by

$$p = (N_A N_V)^{1/2} \exp(-\Delta E_A/2kT), \quad (1)$$

and with both acceptor and donor this is given by

$$p = \frac{(N_A - N_D)N_V}{2N_D} \exp(-\Delta E_A/kT). \quad (2)$$

Here $\Delta E_A$ is the thermal ionization energy of the acceptor, $N_v$ is effective numbers of states in the valence band, while $N_A$ and $N_D$ are the concentrations of acceptor and donor, respectively.[15] Although no impurity band is visible in the calculated energy band structures, in practice there are acceptor and donor levels related to Mg and Si impurities, respectively. To simplify the comparison of numerical results, we assume that the Mg-related acceptor level does not follow the valence band but pins to the vacuum level, as shown by dashed lines in Fig. 3. We approximate the Mg-related acceptor activation energy $\Delta E_{AI}=0.060$ eV, measured in Mg-Si codoped GaN (Ref. 4) as the energy difference between the level and the top of the valence band of configuration I. Then the energy differences between the level and $E_v$ are $\Delta E_{AII}=(0.423+0.060)$ eV$-0.192$ eV$=0.291$ eV for configuration II and $\Delta E_{AMg}=0.423$ eV$+0.060$ eV $=0.483$ eV for Mg-doped GaN. The acceptor activation energy is estimated to be $\Delta E_{AMg}/2=0.241$ eV for Mg-doped GaN, which agrees with the experimental results in the literatures.[16–19] Assume the hole concentrations are $p_I$, $p_{II}$, and $p_{Mg}$ in configurations I, II, and Mg-doped GaN. Then their ratios at room temperature according to Eqs. (1) and (2) are approximately $p_I/p_{Mg} \propto \exp(-\Delta E_{AI}/kT)/\exp(-\Delta E_{AMg}/2kT) \approx 10^3$ and $p_{II}/p_{Mg} \propto \exp(-\Delta E_{AII}/kT)/\exp(-\Delta E_{AMg}/2kT) \approx 0.1$, where $T=300$ K and the ionization energies at room temperature have been corrected by Varnish's law: $E_g=3.427$ eV$-9.39\times10^{-4}$ $T^2/(T+772)$ eV.[20] In practice, the hole concentration of the Mg-doped GaN is about $10^{17}$ cm$^{-3}$.[17–20] The hole concentration of configuration I can thus be enhanced up to $10^{20}$ cm$^{-3}$ even the Si-related donor level concurs. This agrees with the experimental process where Mg was supplied in one pulse and then followed by a Si pulse during crystal growing in the [0001] direction.[4]

## IV. CONCLUSIONS

In conclusion, the charge densities were found to redistribute and concentrate in the N-Mg bonds of configuration I. $E_v$ is thus split widely and shifted up towards the conduction band. This is mainly attributed to the increase of the polarizability strengthened by the parallel component of the local polarized field of configuration I. The N atoms bonding to Mg are found to be as important as Mg for the formation of $E_v$. The electronic structure shifts for configuration I can enhance the hole concentration about $10^3$ times higher than that of Mg-doped GaN.

## ACKNOWLEDGMENTS

The authors would like to express thanks to Professor Zizhong Zhu and Dr. Hui Fang of Xiamen University, and Professor R. Guertin and Dr. Ch. Liu of Tufts University for helpful discussions. This work was partly supported by the Special Funds for Major State Basic Research Projects (Grant No. 001CB610505), the National Nature Science Foundation (Grant Nos. 60376015, 90206030, and 10134030), and grants from the Ministry of Education, Fujian Province (2004H054 and E0410007), and Xiamen of China.

*Author to whom correspondence should be addressed. Electronic address: jykang@xmu.edu.cn

[1] L. Liu and J. H. Edgar, Mater. Sci. Eng., R. **37**, 61 (2002).
[2] A. Yasan and M. Razeghi, Solid-State Electron. **47**, 303 (2003).
[3] Cheul-Ro Lee, Jae-Young Leem, and Byung-Guk Ahn, J. Cryst. Growth **216**, 62 (2000).
[4] S. Iwai, H. Hirayama, and Y. Aoyagi, MRS Proc. Vol. 719 of Defect and Impurity Engineered Semiconductors and Devices

III, F1.1, 2002, edited by S. Ashok, J. Chevallier, N. M. Johnson, B. L. Sopori and H. Okushi.

[5] R. Piotrzkowski, E. Litwin-Staszewska, T. Suski, and I. Grzegory, Physica B **308–310**, 47 (2001).

[6] C. Stampfl, J. Neugebauer, and C. G. Van de Walle, Mater. Sci. Eng., B **59**, 253 (1999).

[7] I. Gorczyca, A. Svane, and N. E. Christensen, Phys. Rev. B **60**, 8147 (1999).

[8] J. E. Northrup, Appl. Phys. Lett. **82**, 2278 (2003).

[9] H. Katayama-Yoshida, R. Kato, and T. Yamaoto, J. Cryst. Growth **231**, 428 (2001).

[10] T. Yamamoto and H. Katayama-Yoshida, J. Cryst. Growth **189/190**, 532 (1998); Jpn. J. Appl. Phys., Part 1 **36**, L180 (1997).

[11] K. S. Kim, G. M. Yang, and H. J. Lee, Solid-State Electron. **43**, 1807 (1999).

[12] D. Cai, J. Kang, and Z. Zhu, Phys. Rev. B **68**, 073305 (2003).

[13] K. Lawniczak-Jablonska, T. Suski, I. Groczyca, N. E. Christensen, J. Libera, J. Kachniarz, P. Lagarde, R. Cortes, and I. Grzegory, Appl. Phys. A: Mater. Sci. Process. **75**, 577 (2002).

[14] Joel I. Gersten and Frederick W. Smith, in *The Physics and Chemistry of Materials* (The City College of the City University of New York, New York, 2001), p. 62.

[15] P. S. Kireev, in *Semiconductor Physics* (Moscow, MIR, 1978), pp. 197–221.

[16] D. Seghier and H. P. Gislason, J. Appl. Phys. **88**, 6483 (2000).

[17] W. Kim, A. Salvador, A. E. Botchkarev, O. Aktas, S. N. Mohammad, and H. Morcoc, Appl. Phys. Lett. **69**, 559 (1996).

[18] B. Z. Qu, Q. S. Zhu, X. H. Sun, S. K. Wan, Z. G. Wang, H. Nagai, Y. Kawaguchi, K. Hiramatsu, and N. Sawaki, J. Vac. Sci. Technol. A **21**, 838 (2003).

[19] M. G. Cheong, K. S. Kim, C. S. Kim, R. J. Choi, H. S. Yoon, N. W. Namgung, E.-K. Suh, and H. J. Lee, Appl. Phys. Lett. **80**, 1001 (2001).

[20] H. Teisseyer, P. Perlin, T. Suski, I. Grzegory, S. Porowski, J. Jun, A. Pietraszko, and T. D. Moustakas, J. Appl. Phys. **76**, 2429 (1994).